Geochemistry of Neoproterozoic Nagod Limestones from the Girgita Mine, Bhander Group, Madhya Pradesh, India

Ravendra Singh, Gyanendra Pratap Singh, and H.U. Usmani

Department of Geology, Government Motilal Vigyan Mahavidyalaya, Bhopal Madhya Pradesh India – 462008
E-mail: thakur.ravendrasingh@gmail.com

ABSTRACT

Vindhyan limestone of the Bander Group (Late Neoproterozoic) in the Maihar area, Satna district, is a part of an anticlinal fold and it forms an outlier in the study area. Geochemical analysis reveals that the proportion of Rare Earth Elements (REEs; La-Lu) in limestones varies between 14.8 ppm and 49.5 ppm. The Eu and Ce anomalies (normalized against Post Archean Australian Shale; PAAS) range from ~ 0.53 to 0.69 and ~ 0.57 to 1.07, respectively. The results of this study revealed that the limestones were principally controlled by the admixture of detrital materials, i.e., (i) The low values of REEs (ii) high values of Y/Ho (iii) positive correlation between REEs and Si, Al, Ti, V, Co, Ni, and Nb, and (iv) slightly negative correlation between CaO and REEs. Further, the variations in Ce anomaly may be due to the influx of detrital materials and positive Ce anomaly was attributable to the shallow marine depositional condition. The distribution of REEs (Chondrite normalized values) illustrates different patterns in the Nagod limestone due to the degree of differentiation in terms of LREEs and HREEs and Eu anomaly. The variations in elemental concentrations and the REE patterns revealed the mixing of detrital materials in the Nagod limestones.

KEY WORDS: Rare Earth Elements, Geochemistry, Nagod limestone, Bhander Group, Vindhyan limestone.

INTRODUCTION

The behavior and mode of distribution of REEs in carbonate rocks have extensively been investigated earlier by many researchers. The studies showed that the important factors influencing enrichment and depletion of REEs in carbonate rocks are: (1) the lithology and diagenesis (Madhavaraju and Ramasamy, 1999), (2) biogenic deposition from seawater (Murphy and Dymond, 1984), (3) scavenging processes related to depth, salinity, and oxygen level of seawater (Greaves et al., 1999), (4) the variation in oxygen level of seawater (Liu et al., 1988), (5) the amount of detrital material of terrigenous origin (Piper, 1974; McLennan,1989; Nagarajan et al., 2011), and (6) the variation in surface productivity. The results of recent investigations revealed that geochemical studies on REEs in carbonate rocks, furnish a suitable basis for reconstruction of paleogeographic conditions, environment of deposition and source of sediments.
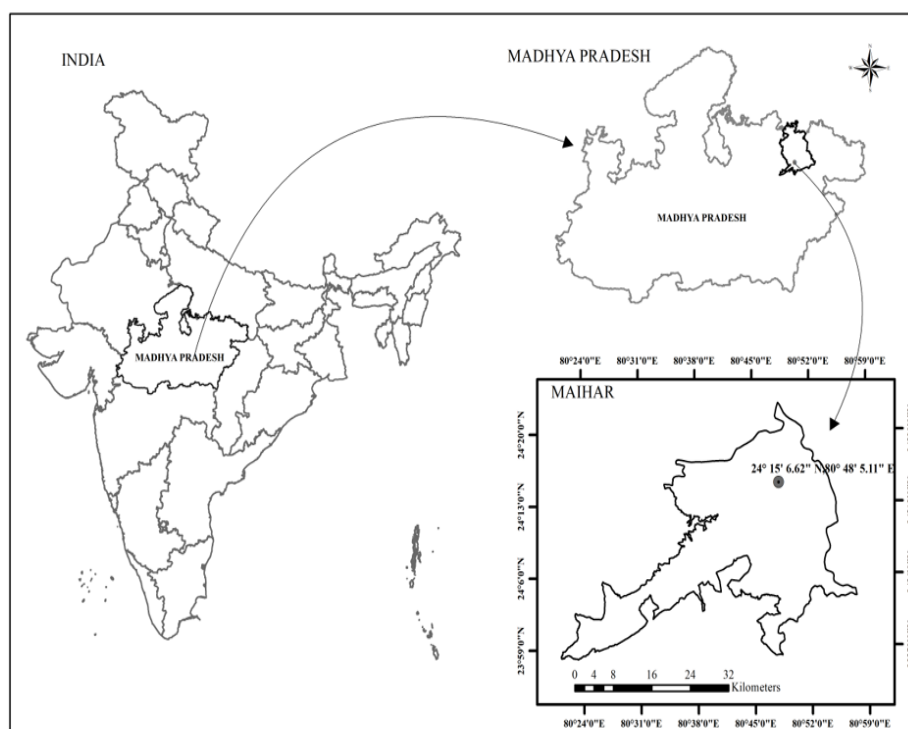

Fig. 1. Location map of the study area.

The Bhander group is widespread to the North of Satna district. The Bihad River flows amidst this limestone belt of Maihar and forms the Chachai Fall down stream. The limestone Fold Belt turns westward from Rewa city and goes westward North of Satna city. In this area, limestone mining is being done by many companies for cement, viz. JP cement, Birla cement, Revati cement, KJS cement plant etc.

The geological map of the study area is shown in Figs. 1 and 2. There are many limestone mines in the Maihar area. The limestone being exploited from Girgita mine is rich in cement grade. A generalized stratigraphic succession of the Vindhyan Supergroup exposed in Maihar area has been given in Fig. 3. Geochemical study of carbonate rocks of the Nagod Formation has been undertaken to investigate the source of REEs and the variations in Eu and Ce anomalies.

Fig. 2. Geological map of the study area.

GEOLOGICAL SETTING

The study area lies on the Survey of India Toposheet Numbers 63D/15, 63D/16. It is limited by Longitude 80°21′15″ E – 80°57′33″ E and Latitude 24°22′45″ N - 23°58′10″ N (Fig. 1). The Girgita mine is Located 12 km east of Maihar city of Satna district.

The Vindhyan basin is a sickle-shaped basin in the Bundelkhand-Aravalli Province which got stabilized prior to 2.5 Ga. The Vindhyan Supergroup overlies a variety of Precambrian basement rocks comprising Bundelkhand Granite, Mahakoshal Group, Bijawar Group, Gwalior Group, Banded Gneissic Complex (BGC) and Chhota Nagpur Gneissic Complex (CGC). The BGC separates the Vindhyan exposures of the Son Valley area from that of the Chambal Valley. The BGC is dominated by K-rich granite emplaced within the Tonalite-Trondjhemite-Granodiorite (TTG) complex. The BGC and Gwalior Group form the basement of Vindhyan Supergroup in the Rajasthan sector. The CGC, consisting of gneisses, granites and granodiorites with enclaves of tonalitic gneisses and ultramafic rocks, forms the basement of the Vindhyan basin in most parts of the eastern Son Valley area.

Sedimentary litho-units in the Vindhyan Basin represent shallow marine facies along with distal shelf to deep-water sediments. The maximum thickness of the entire Vindhyan Supergroup; consisting of sandstone, shale and limestone, is estimated to be around 5 km. and is divisible as shown in Fig. 3.
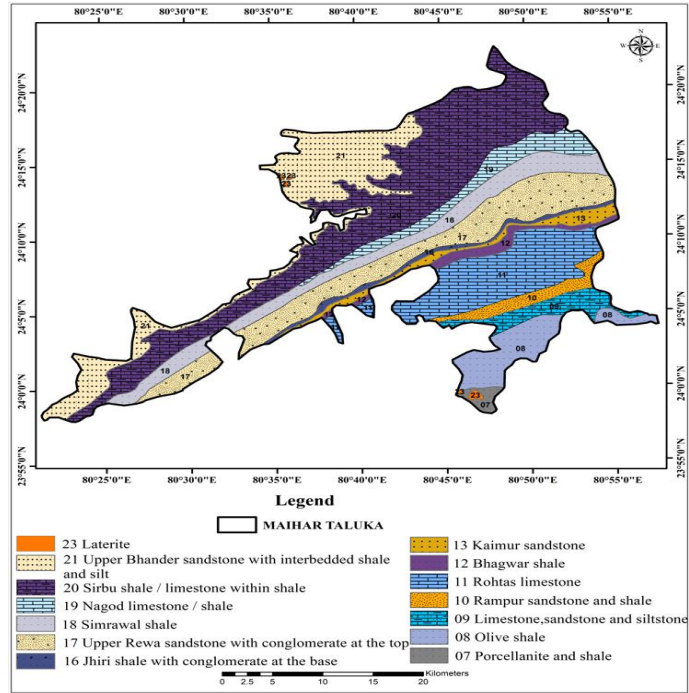
The surface expression of this limestone displays Karstic erosion which is recognizable by the presence of various karst features. The oldest lithologic units in the area are porcellanite shale overlain by olive shale of the Semri Group (Lower Vindhyan). The porcellanite shale contains light gray, greenish yellow, compact and jointed porcellanite with gray to khaki gray splintery shale. Olive shale is olive green in color, fine-grained, hard compact and thinly laminated. Semri Group limestone is dark greyish blue, thickly to thinly bedded. Sandstone of Semri Group is ferruginous, purple, flaggy, and fine to medium-grained. Rampur sandstone is light green, fine-grained, thinly bedded, compact sandstone with tiny grains of bluish green glauconite and gray to khaki gray splintery shale.

Rohtas limestone is light to dark gray, fine-grained, compact and bedded blended with sandy and shaly interbeds. Bhagwar shale is yellowish, carbonaceous, micaceous and pyritiferous. Kaimur Sandstone is fine-grained, massive, hard and thickly bedded. Jhiri shale of Rewa Group (Early Neo-Proterozoic age), is soft, reddish, splintery with interbedded siltstone and thin band of conglomerate at the base. Upper Rewa sandstone with conglomerate at the top, found in the upper part of Jhiri Shale, is reddish brown, hard and massive, coarse grained and thickly bedded. Simrawal shale is soft, purple and reddish brown, thinly laminated to flaggy, calcareous with thin bands of calcite, gypsum interbedded with purplish grey limestone. Nagod limestone is fine grained, hard compact,

thinly bedded to massive with few stromatolitic bands and interbedded with khaki green shale. Sirbhu shale is purple and olive green, thinly laminated silty shale interbedded with bluish grey limestone within shale.

Upper Bhander sandstone is purple to reddish brown, fine to medium-grained and flaggy to massive. Laterite is reddish brown, hard and massive rock which is preserved in the upper most part of Maihar area (Fig. 2).
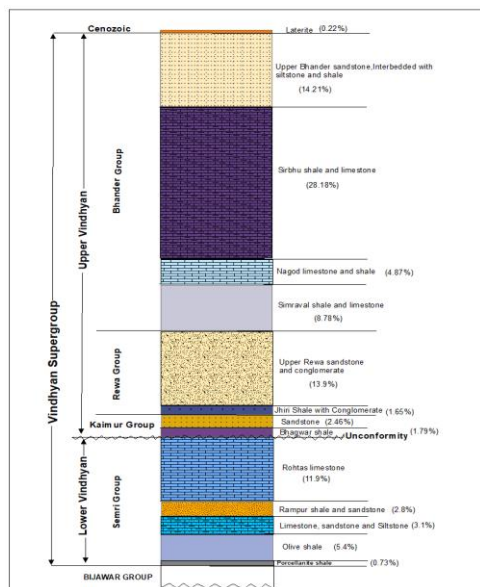

Fig. 3. Stratigraphic succession of the Bijawar Group.

METHODOLOGY

Sampling of Nagod limestone has been carried out at regular vertical interval from the Girgita Mine (Lat. 24°15′7″ N; Long. 80°48′5.11″ E) shown in (Fig. 4). Totally, twelve representative samples have been chosen for chemical analyses. The selected samples were first washed by distilled water to remove contamination and then were air-dried and ground to <2.60 mesh in a tungsten carbide mortar. The powdered samples were analyzed at IIT, Kanpur using ICPMS for REEs, with high quality of analytical precision. The X-Ray Fluorescence Spectroscopy (XRF) analyses of powdered sample were done at the Savitribai Phule University, Pune for trace and major oxide concentrations. Loss on Ignition (LOI) was measured by the loss in dry weight. The results of the values of REEs were normalized to PASS values using the following relation: $Eu/Eu^* = Eu_N/[(Sm_N \times Gd_N)]^{1/2}$ and $Ce/Ce^* = 2Ce_N/(La_N + Pr_N)$, (Where $_N$ stands for the

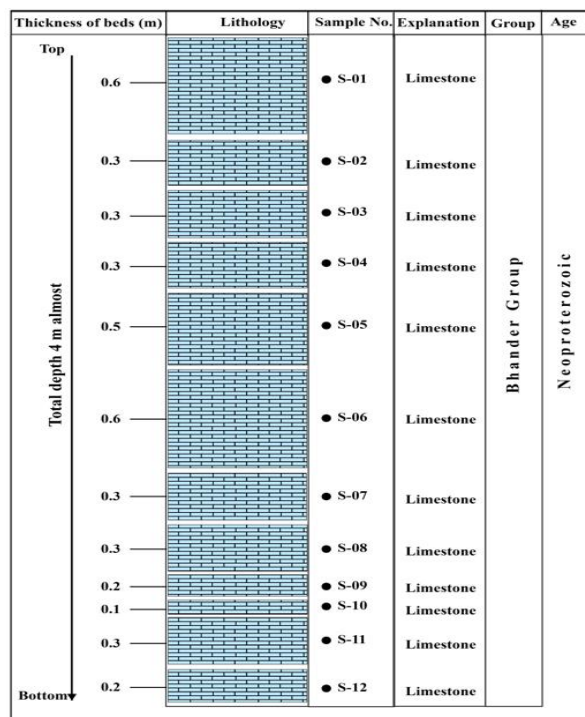normalization of REEs to PAAS; (Taylor and McLennan, 1985).

Fig. 4. Lithology map showing sample locations.

RESULTS

The major, trace and REE concentrations in limestones are listed in Table 1: The bivariate plots between the pairs of major oxides show strong and positive correlations between Al_2O_3 and SiO_2 (r = 0.70), Fe_2O_3 and SiO_2 (r = 0.73), Al_2O_3 and TiO_2 (r = 0.93), Fe_2O_3 and TiO_2 (r = 0.60), and SiO_2 and TiO_2 (r = 0.66). The bivariate plots of major oxide show weak and negative correlations, i.e., Al_2O_3 – CaO (r = -0.70), Fe_2O_3 – CaO (r = -0.58), and CaO– SiO_2 (r = -0.88). The samples show strong depletion in elements such as V, Cr, Co, Ni, Cu, Rb, Y, Nb, and Hf. Strong enrichment for elements like Sr and rather notable enrichment for Ba and Zr is observed (Fig. 5). The REE values for all the analyzed REEs have a range of 14.77 to 49.55 ppm. The chondrite normalized REE patterns are shown in Fig. 6, which reveals enrichment in Ce and Nd contents. The Eu/Eu^* and Ce/Ce^* ratio values vary between 0.53– 0.69 and 0.57–1.07, respectively. The values of Er/Nd and Y/Ho are also within the range of 0.08– 0.12 and 27.62–197.46, respectively. The REEs, in general, have positive correlations with certain major and trace elements such as SiO_2, TiO_2, V, Co, Ni, Rb, and Nb.

Bottom	←					Sample number			→	Top		
Major elements wt. %												
SiO_2	2.92	12.82	15.30	14.75	9.12	12.55	21.95	4.59	18.89	5.58	20.09	10.48
Al_2O_3	0.68	2.41	3.25	2.74	1.31	2.27	2.07	1.00	1.92	0.89	2.17	1.87
K_2O	0.07	0.48	0.66	0.50	0.17	0.49	0.40	0.15	0.37	0.11	0.41	0.30
CaO	55.01	39.21	38.19	42.81	47.09	46.34	34.63	50.62	32.23	53.44	43.78	47.38
TiO_2	0.05	0.19	0.24	0.14	0.10	0.17	0.16	0.06	0.12	0.05	0.13	0.12
Na_2O	BDL	BDL	BDL	BDL	BDL	BDL	BDL	BDL	BDL	BDL	BDL	BDL
MgO	2.13	5.89	8.45	12.65	6.87	1.85	8.41	4.51	11.85	1.54	4.34	2.97
P_2O_5	BDL	0.03	0.04	0.03	0.02	0.03	0.04	BDL	0.02	BDL	0.03	BDL
MnO	0.02	0.03	0.03	0.03	0.06	0.04	0.03	0.02	0.04	0.03	0.04	0.07
Fe_2O_3	0.36	0.87	1.31	1.09	1.33	1.25	1.26	0.60	1.18	0.80	1.35	1.29
LOI	37.15	39.82	36.78	28.87	35.99	37.21	35.33	37.73	38.57	37.04	30.08	37.10
sum	98.39	101.74	104.00	103.61	102.06	102.19	104.29	99.27	105.20	99.48	102.40	102.58
Trace elements (ppm)												
Li	9.82	36.08	46.49	35.27	22.43	26.38	37.85	16.53	37.99	15.30	30.34	29.85
Be	0.11	0.47	0.60	0.39	0.28	0.53	0.36	0.19	0.34	0.18	0.40	0.36
V	4.55	19.80	20.84	15.00	9.62	18.69	14.64	8.76	13.24	8.42	14.31	15.55
Cr	3.94	18.31	19.03	12.61	8.61	16.25	13.47	5.90	11.89	5.64	11.96	12.66
Mn	125.0	215.3	216.9	226.9	390.2	289.7	239.0	148.5	320.6	232.2	270.2	582.9
Co	1.28	2.97	3.24	2.61	2.99	3.21	1.94	1.76	2.48	1.95	2.65	4.90
Ni	6.37	9.08	11.29	8.89	8.31	13.61	7.60	6.85	7.34	7.92	11.83	14.16
Cu	1.47	4.37	6.53	4.44	3.25	4.88	16.23	2.33	4.59	2.64	3.66	5.38
Zn	-0.90	5.34	8.64	8.85	3.40	10.22	12.85	8.26	8.01	6.35	10.40	5.46
Ga	0.80	3.24	4.08	2.58	1.70	3.26	2.79	1.26	2.43	1.19	2.65	2.49
Ge	0.32	0.82	1.00	0.86	0.88	1.13	0.93	0.56	0.77	0.57	1.00	0.87
As	0.88	1.66	1.06	1.78	2.36	3.65	1.93	1.01	1.45	2.27	2.47	3.51
Se	0.98	2.94	0.55	1.96	1.03	0.99	1.15	1.11	0.50	1.42	0.69	1.47
Rb	6.13	25.82	33.12	20.69	11.23	25.07	21.21	9.95	19.28	8.25	20.12	17.04
Sr	441.1	316.6	252.4	253.0	155.4	272.3	231.0	246.0	242.3	241.0	170.8	209.1
Y	2.30	5.30	6.50	7.70	7.00	10.50	5.30	4.40	3.80	4.90	7.10	36.36
Zr	10.17	38.70	47.40	23.70	25.57	31.04	39.90	10.44	20.08	12.19	25.72	24.13
Nb	0.56	2.39	2.79	1.57	1.10	1.97	1.98	0.99	1.37	0.65	1.48	1.34
Mo	0.15	0.14	0.12	0.18	0.16	0.12	0.14	0.15	0.16	0.16	0.19	0.16
Cd	0.02	0.03	0.04	0.03	0.04	0.08	0.08	0.02	0.03	0.04	0.06	0.06
In	-0.85	-0.72	-0.44	-0.49	-0.37	-0.01	-0.11	-0.65	0.27	-0.46	-0.31	-0.35
Sn	0.08	0.55	0.65	0.50	0.28	0.62	0.91	0.14	0.48	0.17	0.51	0.36
Sb	0.06	0.13	0.13	0.11	0.15	0.18	0.19	0.09	0.12	0.13	0.16	0.24
Ba	17.62	49.04	51.94	37.17	66.80	59.77	47.81	16.48	127.62	31.11	47.06	104.75
Hf	0.28	0.99	1.17	0.59	0.59	0.77	0.90	0.25	0.46	0.27	0.59	0.59
Ta	0.05	0.22	0.25	0.13	0.09	0.15	0.15	0.07	0.11	0.05	0.11	0.11
W	0.25	1.44	0.70	0.61	1.14	0.67	0.47	3.31	0.46	0.36	0.73	0.87
Tl	0.08	0.21	0.26	0.16	0.08	0.13	0.12	0.07	0.13	0.07	0.10	0.09
Pb	1.86	5.17	5.57	3.81	3.46	5.43	5.62	3.17	2.69	4.58	3.32	4.49
Bi	0.03	0.06	0.07	0.05	0.03	0.06	0.05	0.03	0.04	0.03	0.03	0.04
S	1012.0	1217.0	2507.0	1903.0	348.7	135.5	581.4	609.1	751.7	121.0	197.9	147.7
Cl	123.0	142.4	156.0	221.7	108.4	62.3	194.0	96.0	254.4	59.1	104.4	158.2
Br	3.00	1.90	2.40	3.20	1.70	2.30	3.00	1.30	2.20	1.90	2.00	3.52
Y	2.30	5.30	6.50	7.70	7.00	10.50	5.30	4.40	3.80	4.90	7.10	36.36
Rare earth elements (ppm)												
La	3.0	5.4	5.9	5.7	5.4	13.4	5.1	3.9	4.0	4.6	7.5	6.3
Ce	6.1	10.4	11.3	12.2	11.1	15.0	9.6	8.9	7.8	10.6	10.7	10.6
Pr	0.7	1.2	1.3	1.5	1.4	2.8	1.1	1.1	0.9	1.2	1.4	1.4
Nd	2.7	4.6	4.8	5.8	5.2	10.3	4.0	4.1	3.4	4.7	5.4	5.3
Sm	0.5	0.9	1.0	1.2	1.1	1.9	0.8	0.8	0.7	1.0	1.0	1.1
Eu	0.1	0.2	0.2	0.2	0.2	0.4	0.2	0.1	0.2	0.2	0.2	0.2

Gd	0.6	1.0	1.0	1.1	1.1	1.9	0.8	0.8	0.7	1.0	1.1	1.1
Tb	0.1	0.1	0.1	0.2	0.2	0.3	0.1	0.1	0.1	0.1	0.1	0.2
Dy	0.4	0.8	0.9	0.9	1.0	1.5	0.7	0.6	0.6	0.8	0.8	0.9
Ho	0.1	0.2	0.2	0.2	0.2	0.3	0.1	0.1	0.1	0.1	0.2	0.2
Er	0.2	0.5	0.6	0.6	0.6	0.8	0.4	0.3	0.3	0.4	0.5	0.5
Tm	0.0	0.1	0.1	0.1	0.1	0.1	0.1	0.0	0.0	0.0	0.1	0.1
Yb	0.2	0.5	0.6	0.5	0.5	0.8	0.4	0.3	0.3	0.3	0.4	0.5
Lu	0.0	0.1	0.1	0.1	0.1	0.1	0.1	0.0	0.0	0.0	0.1	0.1
REE	14.8	26.0	28.1	30.3	28.0	49.6	23.6	21.3	19.1	25.3	29.5	28.3
Eu/Eu*	0.5	0.6	0.6	0.6	0.6	0.6	0.6	0.6	0.7	0.6	0.6	0.6
Ce/Ce*	1.0	1.0	1.0	1.0	1.0	0.6	1.0	1.1	1.0	1.1	0.7	0.8
Er/Nd	0.1	0.1	0.1	0.1	0.1	0.1	0.1	0.1	0.1	0.1	0.1	0.1
Y/Ho	27.6	30.3	34.9	40.0	37.8	35.6	36.6	36.3	33.6	34.1	43.8	197.5

DISCUSSION

The distribution of REEs in calcareous sediments and oceanic water has been discussed by Madhavaraju and Ramasamy (1999). Low concentration of REEs in limestones (average 26.9) is attributed to marine carbonate phase rather than that of clay which generally contains higher average REE concentration as suggested by Piper (1974).

CaO. The positive correlation between REEs and P_2O_5 (r = 0.40; Fig. 7a) depicts that in addition to terrigenous origin for REEs in the limestone, the diagenetic fluids also might have played an effective role in their supply. The mean analytical value of Al_2O_3 in the limestone at Girgita mines is 1.87 wt. %, which is greater than the average value of siliciclastic-contaminated limestones (0.42 wt. %; Veizer, 1983). This concentration value shows
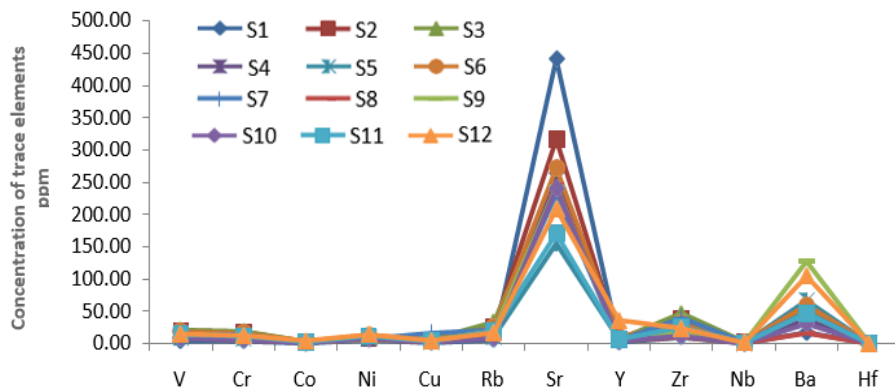

Fig. 5. Distribution patterns of trace elements in the limestone at Girgita mine, Maihar (normalized against UCC).

Bellanca et al. (1997) documented ~ 28 ppm REE average value for marine carbonate rocks. The average REE value of the limestone (26.9) is well comparable with those of Bellanca et al. (1997).

Commonly, REEs with detrital origin have positive correlations with elements such as SiO_2, TiO_2, Al, K, Cr, Co, Rb, Y, V, Ni and Nb, and negative correlation with
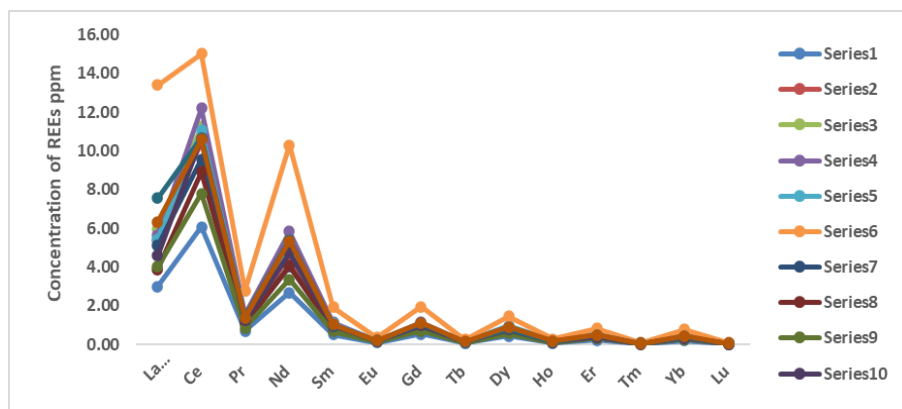

Fig. 6. Distribution patterns of REEs in the limestone at Girgita mine Maihar (normalized against UCC).
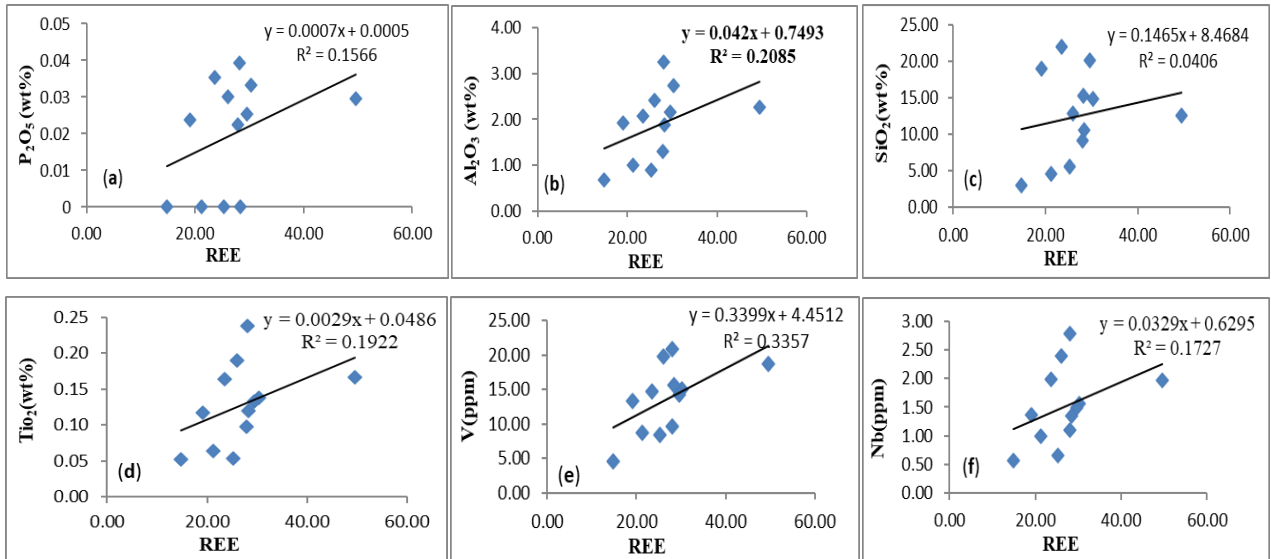
Fig. 7. Bivariate plots between REE and other elements. a) REE-P_2O_5, b) REE-Al_2O_3, c) REE-SiO_2, d) REE-TiO_2, e) REE-V, and f) REE-Nb.
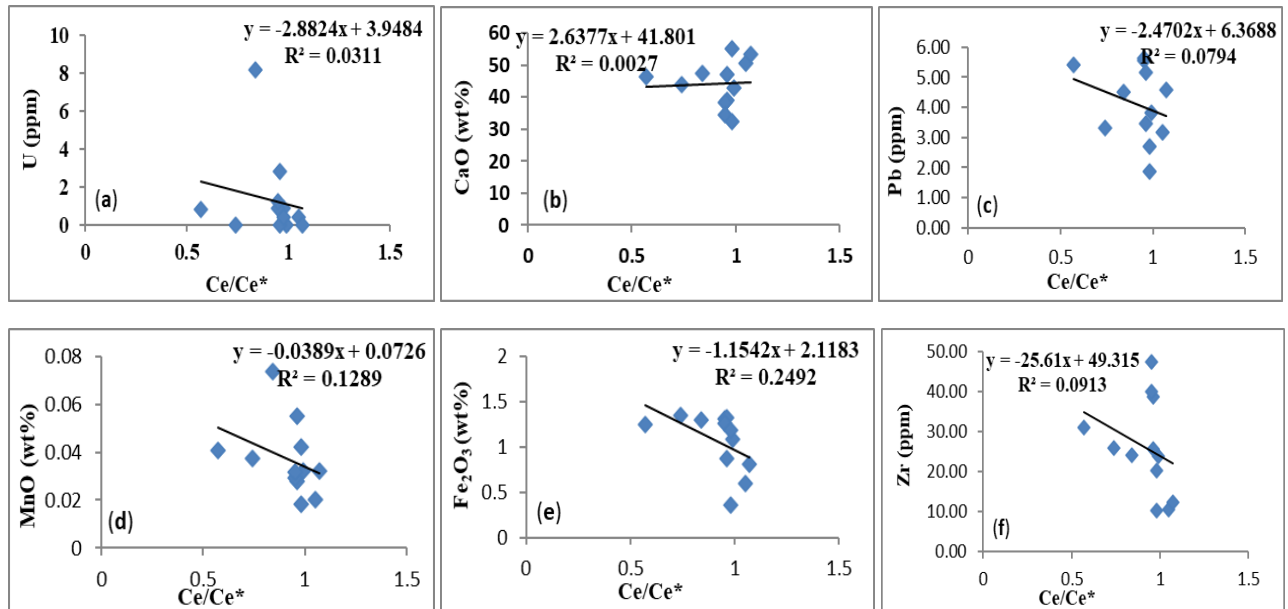

Fig. 8. Bivariate plots: a) Ce/Ce* - U, b) Ce/Ce* – CaO, c) Ce/Ce* – Pb, d) Ce/Ce* – MnO, e) Ce/Ce* – Fe_2O_3, and (f) Ce/Ce* – Zr.

positive correlation with the REE content Al_2O_3 (r = 0.46; Fig. 7b), suggesting an intense contamination (Madhavaraju et al., 2010). This study endorses the terrigenous source for REEs in Nagod limestone by considering the correlation coefficients between REEs and certain major and trace elements.

The Nagod limestone shows that the REEs have a positive correlation with SiO_2 (r = 0.20; Fig. 7c), TiO_2 (r = 0.43; Fig. 7d), V (r = 0.58; Fig. 7e), and Nb (r = 0.42; Fig. 7f). These relations evidently point to a terrigenous derivation of REEs in the Nagod limestone. The positive correlation between MnO and P_2O_5 (r = 0.63) rules out the possibility of significant contamination generated by Mn and Fe oxides in the limestone.

The anomalous values of Ce (Ce/Ce*), in the limestone of the study area, show a narrow range of 0.57–1.07 with an average of 0.92. The Ce anomaly for marine waters ranges from <0.1 to 0.4 (Elderfield and Greave, 1982). Therefore, it appears that the Ce/Ce* values in the Nagod limestone are influenced by the relative proportions of precipitates derived from both pure seawater (carbonates) and suspended fluvial materials. Commonly, the positive anomaly of Ce is generated as a result of influx of terrigenous material (Nath et al., 1992; Madhavaraju and Ramasamy, 1999; Armstrong-Altrin et al., 2003).

Besides, factors like paleo-redox (Liu et al., 1988; German and Elderfield, 1990; Armstrong-

Altrin et al., 2003), fluviatile colloids enriched by Fe-organics (Sholkovitz,1992), and scavenging processes (Masuzawa and Koyama, 1989) could have played crucial role in the occurrence of positive Ce anomalies. The Ce/Ce* values display negative correlation with U (r = –0.2; Fig. 8a) and positive correlation with CaO (r = 0.05; Fig. 8b), indicating that the variations in Ce anomalies are not related to the paleo-redox conditions of the depositional environment. The Ce/Ce* values also have negative correlations with reactive scavenging type particles like Pb, Mn and Fe (r = –0.28 to –0.50; Fig. 8c-8e). These correlations show that the limestone, in question, appears to have been precipitated in a shallow marine environment where the role of scavenging processes is comparatively less than that of deep marine environments. Ce shows positive correlations with elements such as Al (r = 0.53), Ti (r = 0.49), V (r = 0.62), Co (r = 0.51), Ni (r = 0.69), Rb (r = 0.52), Cu (r = 0.09) and Nb (r = 0.47) in the Nagod limestone. The Ce/Ce* values show weak and negative correlations with few major (MnO, CaO, and Fe$_2$O$_3$) and trace elements (U, Zr, and Pb; Fig. 8a-f). So, it can be inferred from these correlations that the Ce abundance and Ce anomalies, in the limestone of the study area, might have been controlled by the influx of detrital materials.

Eu ANOMALY

Eu anomaly values are helpful in comprehending the physico-chemical conditions of various geochemical systems operating in the depositional environment of limestones (Derry and Jacobsen, 1990). The Eu anomalies, in the studied limestone are negative ranging from 0.53 to 0.69, with a mean value of 0.58. Commonly, positive Eu anomalies (normalized to PAAS) are observed in limestones influenced by hydrothermal processes, whereas negative Eu anomaly is indicative of high decomposition of minerals and transportation of minerals containing Eu. Because of the negative correlations between Ce/Ce* and by the presence of components like Fe$_2$O$_3$ and MnO, the role of hydrothermal activities in the occurrenceof positive Eu anomalies, in the limestone at Girgita mines, may be ruled out. Aeolian materials too, have not been reported so far. The role of diagenetic processes can be postulated by positive correlations between Eu/Eu* and by the concentration of certain immobile elements such as Zr, Y and Hf (Madhavaraju and Lee, 2009). The positive correlations between Eu/Eu* and Zr (r = 0.09; Fig. 9a), Eu/Eu* and Y (r = 0.17; Fig. 9b), Eu/Eu* and Th (r = 0.29; Fig. 9c) and Eu/Eu* and Hf (r = 0.04; Fig. 9d) advocate the effective role of diagenesis in the occurrence of Eu anomalies in the Nagod limestone. Furthermore, the effect of diagenetic alteration can be deduced by the strong positive correlation between Mn and Sr (r = -0.56) (Brand and Veizer, 1980). Inclusion of detrital feldspars in sediments can bring about positive Eu anomalies in limestones. The ratios of oxides like Na$_2$O/Al$_2$O$_3$ and K$_2$O/Al$_2$O$_3$ may help in the recognition of different kinds of feldspars in sediments (Madhavaraju and Lee, 2009; Nagarajan et al., 2011). Therefore, it seems that in addition to diagenetic processes, the presence of K-feldspars appears to have played a significant role in the occurrence of negative Eu anomaly in the Nagod limestone.
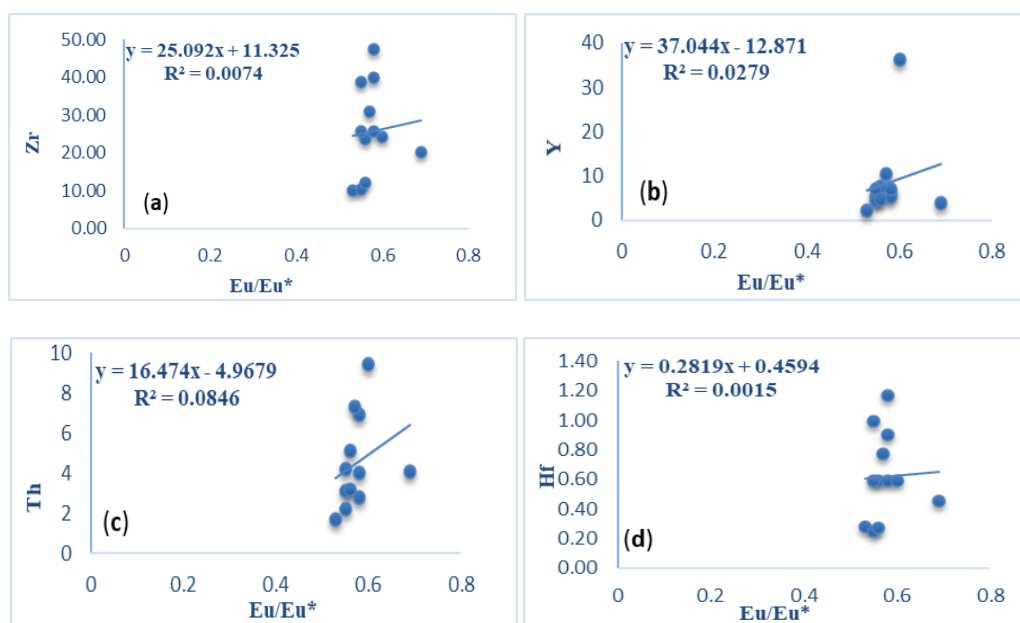

Fig. 9. Bivariate plots: a) Eu/Eu* – Zr, b) Eu/Eu* – Y, c) Eu/Eu* – Th, and d) Eu/Eu* –Hf.

Y / Ho and Er / Nd ELEMENTAL RATIOS

Yttrium(Y) is identical to Ho and Dy in terms of ionic charge and ionic radius. Therefore, in distribution pattern of REEs, it is inserted between Ho and Dy (Bau, 1996). Although Y and Ho have similar geochemical behavior, yet Ho can be removed from sea water twice as fast as Y. This phenomenon is related to the difference in degree of surface complex stabilities, which leads to a notable super chondritic marine ratio of Y/Ho (Bau, 1996; Nozaki et al., 1997). Terrigenous material and volcanic ash have constant chondritic values of Y/Ho (Approximately 28). Seawaters have Y/Ho values greater than those of volcanic ash, ranging from 44 to 74 (Bau, 1996; Nozaki et al., 1997).

In this study, the Nagod limestone has Y/Ho values varying noticeably from 27.62 to 197.46 (mean 49). These values indicate that the limestones are contaminated with terrigenous materials. The ratio value of Er/Nd in normal seawater is ~ 0.27 (De Baar et al., 1988). The Er/Nd value in limestone efficiently indicate the seawater signature. The Er/Nd values, in the studied limestone, display a narrow range of ~ 0.08 - 0.12, which in turn, indicate the effective role of detrital material and diagenetic processes in the occurrence of Er and Nd in the Nagod limestone.

The controlling factor of diagenetic processes in the distribution of REEs in limestones can be established by a negative correlation between Eu/Eu* and Ce/Ce*. The existence of negative correlation between Eu/Eu* and Ce/Ce* (r = 0.006; Fig. 10) demonstrates that the processes during diagenesis are the controlling factor in the distribution of REEs in limestone.

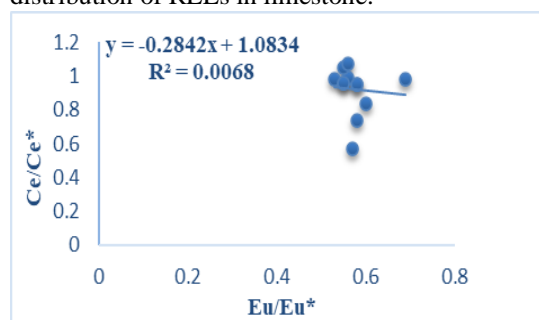Fig. 10. Bivariate plot between Eu/Eu* and Ce/Ce* ratios for the Nagod limestones.

CONCLUSIONS

Geochemical indicators such as low ratio of Y/Ho and high values of REEs suggest that the concentration of REEs in the limestone is associated with the incorporation of terrigenous material. This can further be supported by the positive correlation of REE with elements such as Si, Al, Ti, V, Co, Ni, Rb, Cu and Nb, and by negative correlation between REE and CaO. The positive correlation between Ce/Ce* and Si, Al, Zr, Hf and Y, and along a negative correlation between Ce/Ce* and CaO, U, Fe_2O_3 and MnO reveal that variation in the values of Ce anomalies in the limestone have substantially been controlled by fluvial detrital material. Besides, the negative correlation furnishes strong evidence for the deposition of limestones in a shallow marine environment.

REFERENCES

Armstrong-Altrin, J.S., Verma, S.P., Madhavaraju J, Lee YI, Ramasamy S (2003). Geochemistry of Late Miocene Kudankulam Limestones, South India. International Geology Review, 45:16–26.

Bau, M. (1996). Controls on the Fractionation of Isovalent Trace Elements in Magmatic and Aqueous Systems: Evidence from Y/Ho, Zr/Hf and Lanthanide Tetrad Effect. Contributions to Mineralogy and Petrology, 123:323–333.

Bellanca, A., Masetti, D., Neri, R. (1997). Rare earth elements in limestone/marlstone couplets the Albian-Cenomanian Cismon section (Venetian region, from northern Italy): assessing REE sensitivity to environmental changes. Chemical Geology, 141:141–152.

Brand, U., Veizer, J. (1980). Chemical diagenesis of a multi component carbonate system: trace elements. Journal of Sedimentary Petrology, 50:1219–1236.

De Baar, H.J.W., German, C.G., Elderfield, H., Van-Gaans, P. (1988). Rare earth elements distributions in anoxic waters of the Cariaco Trench. Geochimica et Cosmochimica Acta, 52:1203–1219.

Derry, L.A., Jacobsen, S.B. (1990). The chemical evolution of Precambrian seawater: evidence from REEs in banded iron formations. Geochimica et Cosmochimica Acta, 54:2965–2977.

Elderfield, H., Greaves, M.J. (1982). The rare earth elements in seawater. Nature, 296:214–219.

German, C.R., Elderfield, H. (1990). Application of Ce anomaly as a paleo-redox indicator: the ground rules. Paleoceanography, 5:823–833.

Greaves, M.J., Elderfield, H., Sholkovitz, E.R. (1999). Aeolian sources of rare earth elements to the Western Pacific Ocean. Marine Chemistry, 68:31–38.

Liu, Y.G., Miah, M.R.U., Schmitt, R.A. (1988). Cerium: a chemical tracer for paleooceanic redox conditions. Geochimica et Cosmochimica Acta, 52:1361–1371.

Madhavaraju, J., Gonzalez-Leon, C.M., Lee, Y.I., Armstrong-Altrin, J.S., Reyes-Campero, L.M. (2010). Geochemistry of the Mural Formation (Aptian-Albian) of the Bisbee Group, Northern Sonora, Mexico. Cretaceous Research, 31:400–414.

Madhavaraju, J., Lee, Y. (2009). Geochemistry of the Dalmiapuram Formation of the Uttatur Group (Early Cretaceous), Cauvery basin, southeastern India: implications on provenance and paleo- redox conditions. Revista Mexicana de Ciencias Geologicas, 26:380–394.

Madhavaraju, J., Ramasamy, S. (1999). Rare earth elements in limestones of Kallankurichchi Formation of Ariyalur Group, Tiruchirapalli, Tamil Nadu. Journal of the Geological Society of India, 54:291–301.

Masuzawa, T., Koyama, M. (1989). Settling particles with positive Ce anomalies from the Japan Sea. Geophysical Research Letters 16:503–506.

McLennan, S.M. (1989). Rare earth elements in sedimentary rocks: Influence of provenance and sedimentary processes. In: Lipin BR, McKay GA, editors. Geochemistry and Mineralogy of Rare Earth Elements. Chantilly, VA, USA: Mineralogical Society of America, pp. 169–200.

Murphy, K., Dymond, J. (1984). Rare earth element fluxes and geochemical budget in the eastern equatorial Pacific. Nature 307:444–447.

Nagarajan, R., Madhavaraju, J., Armstrong-Altrin, J.S., Nagendra, R. (2011). Geochemistry of Neoproterozoic limestones of the Shahabad Formation, Bhima Basin, Karnataka, southern India. Geosciences Journal, 15:9–25.

Nath, B.N., Roelandts, I., Sudhakar, M., Pluger, W.L. (1992). Rare Earth Element patterns of the Central Indian Basin sediments related to their lithology. Geophysical Research Letters, 19:1197–1200.

Nozaki, Y., Zhang, J., Amakawa, H. (1997). The fractionation between Y and Ho in the marine environment. Earth and Planetary Science Letters, 148:329–340.

Piper, D.Z. (1974). Rare earth elements in the Sedimentary cycle: a summary. Chemical Geology, 14:285–304.

Sholkovitz, E.R. (1992). Chemical evolution of rare earth elements: fractionation between colloidal and solution phases of filtered river water. Earth and Planetary Science Letters, 114:77–84.

Taylor, Y., McLennan, S.M. (1985). The Continental Crust: Its Composition and Evolution. 1st ed. Oxford, UK.

Veizer, J. (1983). Trace elements and isotopes in sedimentary carbonates. In: Reeder RJ, editor. Carbonates: Mineralogy and Chemistry, Vol. 11. Chantilly, VA, USA: Mineralogical Society of America, pp. 265–299.